Materials Letters 99 (2013) 24–27

Contents lists available at SciVerse ScienceDirect

Materials Letters

journal homepage: www.elsevier.com/locate/matlet

# Improving the photo-degradation activity of $SnS_2$ under visible light by $TiO_2$ (rutile)

Feifei Yang, Gaoyi Han*, Dongying Fu, Zhaoyang Liu

*Institute of Molecular Science, Shanxi University, Taiyuan 030006, PR China*

ARTICLE INFO

*Article history:*
Received 5 December 2012
Accepted 5 February 2013
Available online 14 February 2013

*Keywords:*
$SnS_2$
$TiO_2$
Photodegradation
Nanocomposites
Semiconductors

ABSTRACT

The nano-sized $SnS_2$ modified with rutile phase $TiO_2$ ($SnS_2/TiO_2$) was prepared through the hydrothermal treatment of $TiCl_3$ in the presence of $SnS_2$ at 160 °C for 4 h. The samples have been characterized by X-ray diffraction, X-ray photoelectron spectroscopy, scanning and transmission electron microscopy and UV–vis spectroscopy. The photodegradation of methyl orange has been investigated under the light irradiation of 360–600 and 400–600 nm by using the samples as photocatalyst. The results demonstrated that the photocatalytic activities of the as-prepared $SnS_2/TiO_2$ depended on the content of $TiO_2$, and that $SnS_2/TiO_2$ containing 26% $TiO_2$ displayed the optimum activity which was much larger than that of pure $SnS_2$ although the rutile $TiO_2$ had little activity for the degradation of methyl orange.

## 1. Introduction

Recently, there has been considerable interest in the application of semiconductors as photocatalysts to clean environment and produce $H_2$ energy via splitting water. During the process the electron–hole pairs are separated upon irradiation of photons, and then the electrons or holes move to the surfaces and react with species adsorbed on the powders [1]. To date, it has been reported that the composite structure can enhance the photocatalytic activity of the semiconductor catalysts, and that the improved activity of the composites is largely attributed to the enhanced separation of photo-induced electrons and holes via interfacial charge transfer [2–5]. Hence, much effort has been devoted to develop composite semiconductors in order to maximize the utilization of solar energy and reduce the recombination of electron–hole [6].

$SnS_2$, a kind of n-type semiconductor with a bandgap of 2.18–2.44 eV, has good stability in acid and neutral aqueous solutions and some oxidative and thermal stability in air, which makes it a promising visible light-sensitive photocatalyst [7] or dye in photocell [8,9]. Anatase (3.2 eV) crystalline phase $TiO_2$ has been used widely due to its non-toxicity, inexpensiveness and considerable photo-stability [10]. Recently, it was revealed by some reports that rutile $TiO_2$ (3.0 eV) with a small size and large surface area can possess relatively higher photocatalytic activity [11–13] although anatase is usually more active than rutile [14]. Considering the appropriate matching degree of band potentials between $SnS_2$ and rutile $TiO_2$, $SnS_2/TiO_2$ composites with appropriate compositions will have higher visible light-driven photocatalytic activity than individual $SnS_2$ and $TiO_2$.

In this paper, $SnS_2/TiO_2$ composites are prepared by the hydrothermal method in the presence of $SnS_2$ and $TiCl_3$ aqueous solutions. It is proved that the degradation of methyl orange under visible light can be greatly improved when the optimum composite of $SnS_2/TiO_2$ (rutile) is used as catalyst.

## 2. Experimental

*Materials*: All reagents were of analytical grade and $SnS_2$ nanoparticles were synthesized according to literature [7]. The pure $TiO_2$ particles were synthesized by treating 1.0 mL $TiCl_3$ aqueous solutions in 10 mL distilled water at 160 °C for 4 h.

$SnS_2$ powder (120 mg) was dispersed in distilled water, and then certain amount of $TiCl_3$ aqueous solution was dropped into the mixture under stirring. The mixtures were transferred into teflon-lined stainless steel autoclaves, and then the autoclaves were heated at 160 °C for 4 h in an oven. The final products were filtered, washed with distilled water several times, and then dried in a vacuum oven at 100 °C for 3 h. The composite containing 17, 23, 26, 29 and 33 wt% of rutile phase $TiO_2$ was defined as $SnS_2/TiO_2$-17, 23, 26, 29 and 33, respectively.

*Characterization and tests*: The morphologies of the samples were observed by using a scanning electron microscope (SEM, JEOL6701F) and transmission electron microscopy (TEM, JEOL2010). The XRD patterns were recorded on a Bruker D8 Advance X-ray

---

* Corresponding author. Tel./fax: +86 35 1701 6358.
*E-mail address:* han_gaoyis@sxu.edu.cn (G. Han).

0167-577X/$ - see front matter © 2013 Elsevier B.V. All rights reserved.
http://dx.doi.org/10.1016/j.matlet.2013.02.009

diffractometer (Cu Kα), and the X-ray photoelectron spectroscopy (XPS) measurements were performed on an ESCAL-ab 220i-XL spectrometer (VG Scientific, England) employing a monochromic Al Kα source at 1486.6 eV. The UV–vis diffuse diffraction spectra were obtained on a Thermo Scientific Evolution 220 UV–visible spectrophotometer.

Photocatalytic experiments were carried out by using MO (20.0 mg/L) solution as target under the 360–600 and 400–600 nm light irradiation. Before illumination, the mixture of MO (50.0 mL) and photocatalyst (10.0 mg) was magnetically stirred under darkness for 30 min to reach the adsorption/desorption equilibrium. Then the reactions were initiated by irradiating with a 200 W Xe lamp located 36 cm above the vessel; the temperature of the solution was kept at about 25 °C in the process of degradation. During the irradiation, 1.0 mL of the mixture under radiation was taken from the vessel at an interval of 5 or 10 min and was centrifuged at 12,000 rpm for 5 min to remove the catalyst particles completely. The concentration of MO solution was determined by a UV–vis spectrophotometer at the maximum absorption wavelength of 462.0 nm.

## 3. Results and discussion

From the SEM images (Fig. S1), it is difficult to get the shape and size of the particles for $SnS_2$ and $SnS_2/TiO_2$, but it is clear that the pure $SnS_2$ particles are flaky, and that the small $TiO_2$ particles are assembled on the surface of $SnS_2$ in the samples of $SnS_2/TiO_2$–26 (Fig. 1A and B). However, pure $TiO_2$ particles synthesized from $TiCl_3$ exhibit the size of several microns (Fig. 1C). These indicate that $TiO_2$ can disperse on $SnS_2$ well and the composites have been synthesized successfully. The XRD pattern shows the characterized diffraction peaks of pure $SnS_2$ (Fig. 1(D-a)) while the XRD pattern of $TiO_2$ (Fig. 1(D-g)) shows that the rutile $TiO_2$ is synthesized in this approach but without the anatase phase. The XRD patterns of $SnS_2/TiO_2$ composites with various contents of

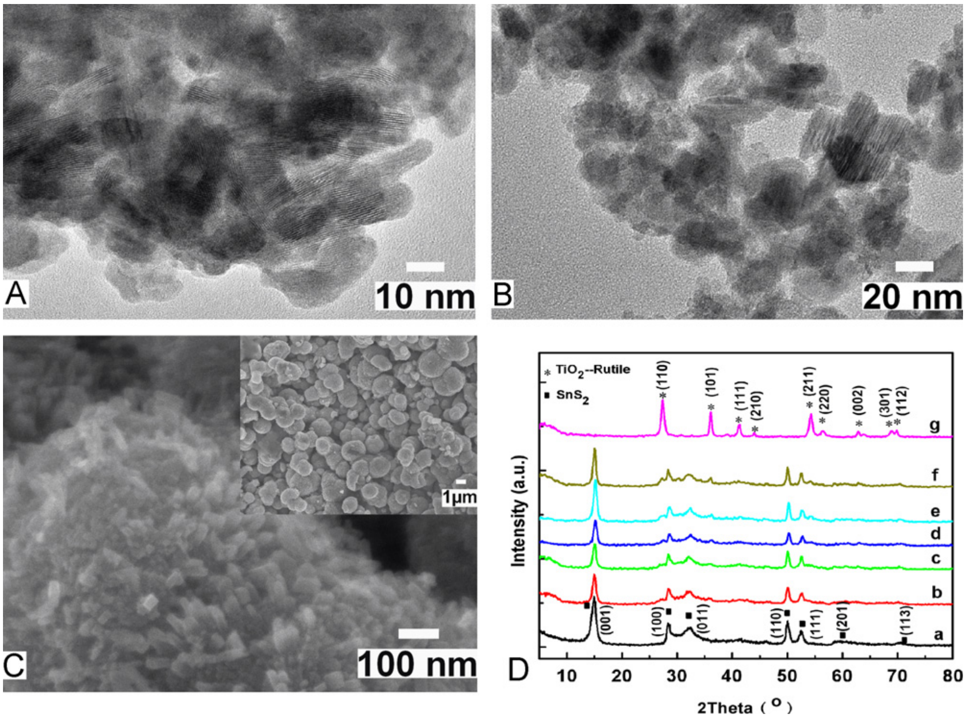

**Fig. 1.** TEM images of pure $SnS_2$ (A) and $SnS_2/TiO_2$-23 (B), the SEM images of pure $TiO_2$ (C) and the XRD patterns of the samples of $SnS_2$ (a), $SnS_2/TiO_2$-17 (b), $SnS_2/TiO_2$-23 (c), $SnS_2/TiO_2$-26 (d), $SnS_2/TiO_2$-29 (e), $SnS_2/TiO_2$-33 (f) and $TiO_2$ (g).

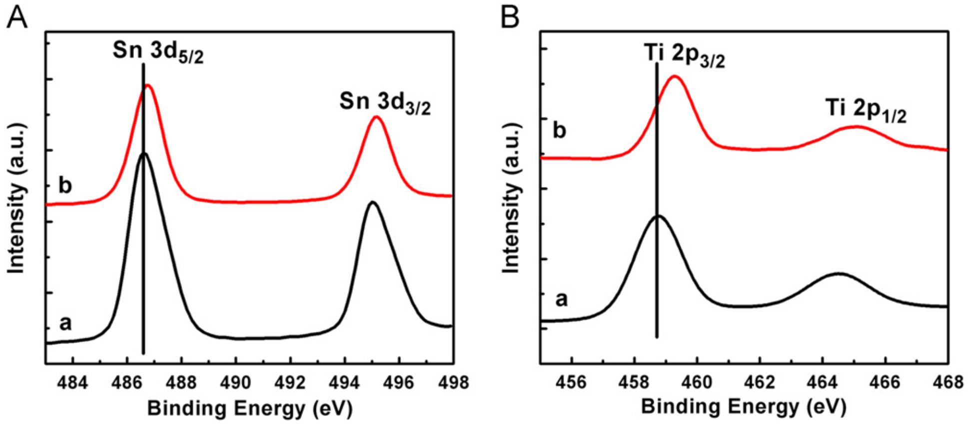

**Fig. 2.** The XPS spectra of Sn3d (A) for $SnS_2$ (a) and $SnS_2/TiO_2$-26 (b), and Ti2p (B) for $TiO_2$ (a) and $SnS_2/TiO_2$-26 (b).

$TiO_2$ possess the peaks corresponding to $SnS_2$ and $TiO_2$. But it is found that the peaks of rutile $TiO_2$ in $SnS_2/TiO_2$-26 have relatively weaker intensity than the mixture of $SnS_2$ and $TiO_2$ with the same ratio (Fig. S3), which may be because the content of rutile $TiO_2$ in composite is less than that of mixture or because the particles of $TiO_2$ deposited on the surface of SnS2 have small size and poor crystallization.

The XPS spectra are recorded in order to clarify the interaction between the components (Fig. 2). The binding energy (BE) of $Sn3d_{5/2}$ (486.7 eV) for $SnS_2/TiO_2$-23 is higher than that for pure $SnS_2$ (486.6 eV), which may be due to some tin oxide (486.9 eV) formed during the preparation process which can cause the BE of $Sn3d_{5/2}$ to shift to higher region [15] compared with pure $SnS_2$. Moreover, the BE of $Ti2p_{3/2}$ for $SnS_2/TiO_2$ is located at 458.6 eV which is also higher than that of rutile $TiO_2$ (458.3 eV). The above-mentioned XPS results reveal that there are changes in the outer electron cloud density of Ti and Sn ions, and that the interaction between $SnS_2$ and $TiO_2$ in the composites is strong.

The UV–vis diffuse reflection spectra of the samples (Fig. 3) reveal that $TiO_2$ displays a strong absorption mainly below 400 nm while $SnS_2$ and $SnS_2/TiO_2$ display light absorption in the wavelength range of 400–750 nm. It is found that the intensity of the absorption in the UV region decreases with the increase of $TiO_2$ in the composites (Fig. 3(A)). In order to confirm this

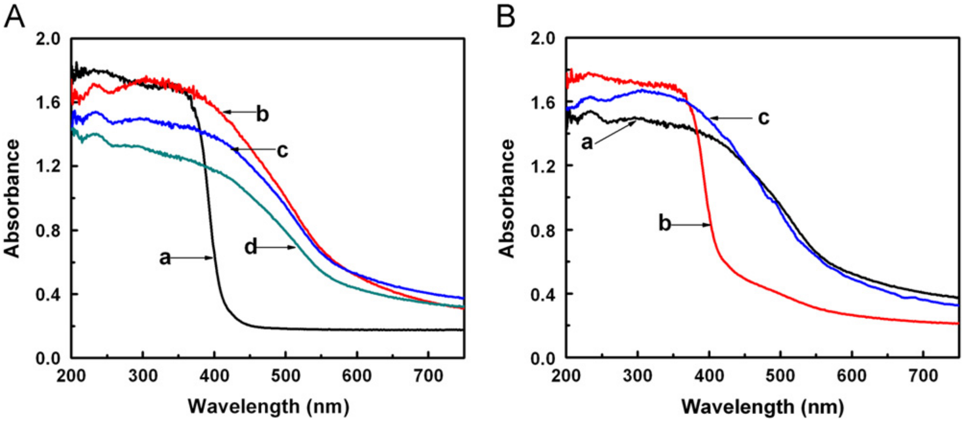

**Fig. 3.** UV–vis diffuse reflection spectra (A) for the sample of $TiO_2$ (a), $SnS_2$ (b), $SnS_2/TiO_2$-23 (c) and $SnS_2/TiO_2$-33 (d) and the curves (B) $SnS_2/TiO_2$-26 (a), the 74% $SnS_2$ spectrum+26% $TiO_2$ spectrum and $SnS_2/TiO_2$-26 (physical mixing) (c).

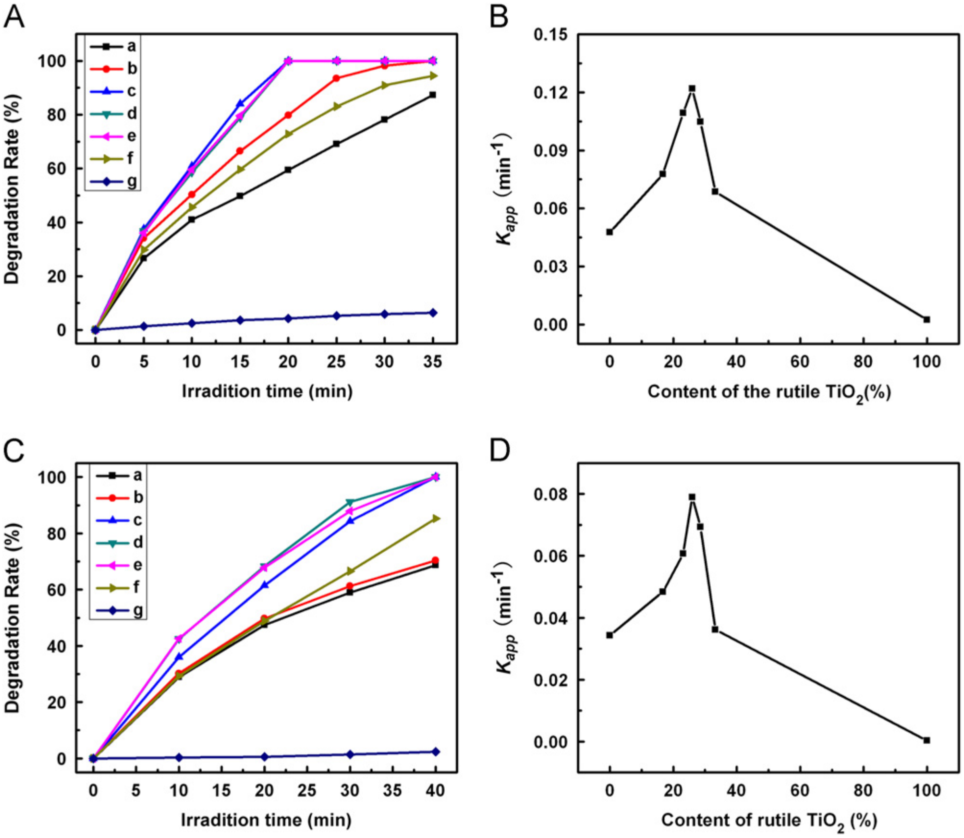

**Fig. 4.** The curves of the degradation for MO in the presence of $SnS_2$ (a), $SnS_2/TiO_2$-17 (b), $SnS_2/TiO_2$-23 (c), $SnS_2/TiO_2$-26 (d), $SnS_2/TiO_2$-29 (e), $SnS_2/TiO_2$33 (f) and $TiO_2$ (g) under 360–600 nm (A) and 400–600 nm (C) and the plots of $K_{app}$ for MO degradation versus the content of $TiO_2$ in the composites under 360–600 nm (B) and 400–600 nm (D).

phenomenon, the electron adsorption spectrum of $SnS_2/TiO_2$-26 (physical mixing) has been recorded and it shows stronger adsorption in the range $<450$ nm and slightly weaker adsorption in the range of 450–750 nm than $SnS_2/TiO_2$-26, which is similar to the curve of 74% $SnS_2$ spectrum+26% $TiO_2$ spectrum but with a relatively stronger absorption in the range of 400–750 nm (Fig. 3B). This may be because the content of rutile in $SnS_2/TiO_2$-26 is less than the mixture, or because the $TiO_2$ dispersed on the surface of $SnS_2$ exhibits a weaker absorption in the UV region than the sole $TiO_2$ due to the small size.

From Fig. 4A and C, it is found that the degradation of MO almost does not take place when $TiO_2$ is used as the photocatalyst under the irradiation of 360–600 nm (1.12%, 20 min) and 400–600 nm (1.16%, 40 min), while it is 59.4% at 20 min (360–600 nm) and 71.6% at 40 min (400–600 nm) when $SnS_2$ is used as photocatalyst. However, the degradation rate is about 100% at 20 min under 360–600 nm and 40 min under 400–600 nm irradiation in the presence of $SnS_2/TiO_2$-23, 26 or 29. The photo-catalytic degradation of the organic pollutants follows the pseudo-first-order kinetic; the apparent reaction constant ($K_{app}$) can be obtained from the linear relationship between $\ln(C_0/C_t)$ and the reaction time. It is clear that the $K_{app}$ in the presence of $SnS_2$ is about 0.048 $min^{-1}$ (360–600 nm) and 0.034 $min^{-1}$ (400–600 nm), and that the $K_{app}$ increases with the increase of $TiO_2$ in composites initially. The $K_{app}$ reaches the maximum (0.12 $min^{-1}$ under 360–600 nm, 0.079 $min^{-1}$ under 400–600 nm) when the content of $TiO_2$ is about 26% in the composite which is much larger than that of $SnS_2$, and decreases when the content of $TiO_2$ in the composites increases further. However, the degradation of the MO is about 96% at 40 min, and the $K_{app}$ is about 0.060 $min^{-1}$ under irradiation of 260–400 nm, which is smaller than that under the irradiation of visible light. So it can be concluded that among these obtained photocatalysts, $SnS_2/TiO_2$-26 reveals the most efficacious performance under the visible light. According to the above measurements, the higher degradation of MO caused by the composite under visible light may be ascribed to the matching band potentials of $SnS_2/TiO_2$ and efficient electron–hole separations via interface.

## 4. Conclusions

$SnS_2/TiO_2$ composites with different contents of $TiO_2$ have been prepared via hydrothermal treatment of various amounts of $TiCl_3$ aqueous solutions in the presence of $SnS_2$ at 160 °C for 4 h. There are intense interactions between the components of the composites, and the activities of $SnS_2/TiO_2$ depend on the mass ratio of the components. Composite of $SnS_2/TiO_2$-26 possesses the optimum photocatalytic activity under UV–visible or visible light irradiation. The high visible light-driven activity makes it a kind of promising catalyst in the efficient utilization of solar energy for the treatment of some chemically organic dye.

## Acknowledgments

The authors thank the funding of NSFC (21274082 and 21073115) and NCET-10-0926 of China.

## Appendix A. Supporting information

Supplementary data associated with this article can be found in the online version at http://dx.doi.org/10.1016/j.matlet.2013.02.009.

## References

[1] Yang CY, Wang WD, Shan ZC, Huang FQ. J Solid State Chem 2009;182:807–12.
[2] Zhang YC, Du ZN, Zhang M. Mater Lett 2011;65:2891–4.
[3] Xie Y, Ali G, Yoo SH, Cho SO. ACS Appl Mater Interfaces 2010;2:2910–4.
[4] Zhang YC, Du ZN, Li KW, Zhang M, Dionysiou DD. ACS Appl Mater Interfaces 2011;3:1528–37.
[5] Zhou W, Liu H, Wang J, Liu D, Du G, Cui J. ACS Appl Mater Interfaces 2010;2:2385–92.
[6] Wang DS, Zhang J, Luo QZ, Li XY, Duan YD, An J. J Hazard Mater 2009;169:546–50.
[7] Zhang YC, Du ZN, Li KW, Zhang M. Sep Purif Technol 2011;81:101–7.
[8] Tsukigase H, Suzuki Y, Berger MH. J Nanosci Nanotechnol 2011;11:3215–21.
[9] Wang Y, Gong H, Fan BH, Hu GX. J Phys Chem C 2010;114:3256–9.
[10] Ling QC, Sun JZ, Zhou QY. Appl Surf Sci 2008;254:3236–41.
[11] Li Y, Lee NH, Lee EG, Song JS, Kim SJ. Chem Phys Lett 2004;389:124–8.
[12] Watson SS, Beydoun D, Scott JA, Amal R. Chem Eng J 2003;95:213–20.
[13] Habibi MH, Vosooghian H. J Photochem Photobiol A 2005;174:45–52.
[14] Yuan MQ, Zhang J, Yan S, Luo GX, Xu Q, Wang X, et al. J Alloys Compd 2011;509:6227–35.
[15] Boppana VBR, Lobo RE. J Catal 2011;281:156–68.